

# The Microwave Spectrum of Oxazole

## II. Dipole Moment and Quadrupole Coupling Constants

Anil Kumar, John Sheridan, and Otto L. Stiefvater

School of Physical and Molecular Sciences, University College of North Wales, Bangor LL57 2UW Gwynedd, U.K.

Z. Naturforsch. **33a**, 549–558 (1978); received February 11, 1978

The dipole moments and the quadrupole coupling constants of the normal and the three mono-deuterated species of oxazole have been measured. The dipole moment of  $1.50 \pm 0.03$  D is found to deviate by  $10.8^\circ$  from the external bisector of the CNC angle towards the C(2) carbon atom. The principal values of the quadrupole coupling tensor are determined as  $\chi_{zz} = -4.04 \pm 0.02$  MHz and  $\chi_{xx} = 1.66 \pm 0.02$  MHz along the axes in the molecular plane, so that the gradient perpendicular to this plane is  $\chi_{yy} = 2.38$  MHz. The direction of the largest gradient deviates by  $5.7^\circ$  from the external bisector of the CNC angle towards the carbon atom C(4).

An attempt is made to correlate these results and the geometry of oxazole with the electron distribution in this molecule.

### I. Introduction

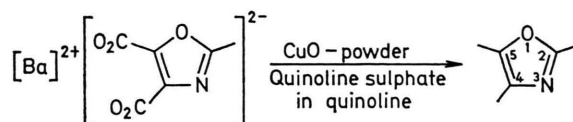
As a first part of the renewed investigation of oxazole by microwave spectroscopy, we reported in a preceding paper [1] the complete substitution structure of this compound as determined by DRM techniques. With this work as a basis, valuable information concerning the electron distribution in oxazole can be deduced by the traditional SEM techniques from the magnitude and orientation of the dipole moment and of the electric field gradients at the site of the nitrogen atom. Accordingly, the present part reports results for the dipole moment and the quadrupole coupling constants of the normal and the three mono-deuterated forms of oxazole, and an attempt is made to correlate this information with the likely electron distribution within the molecule.

### II. Experimental

#### a) Samples

Preliminary work was carried out with a sample of oxazole provided by Professor H. Bredereck and Dr. K. H. W. Turck. Later studies were made with normal and deuterated samples prepared according to the method of Bangert [2]. The final stage of this preparation consisted in the decarboxylation of the barium salt of oxazole-4,5-dicarboxylic acid, from

which a crude sample of oxazole was obtained and purified by distillation:



Deuterium substitution at the 2-position was obtained by direct exchange of oxazole with  $D_2O$ , but the 4- and 5-positions could not be deuterated in this simple way. Hence, in order to obtain the latter two species, it was necessary to introduce the deuterium in the final stage of the preparation given above. To this end, quinoline was treated with  $HDSO_4$  or  $D_2SO_4$  to obtain the quinoline sulphate for use in the decarboxylation of the barium salt. In principle, this was expected to yield the 4- $d_1$ , 5- $d_1$  and the 4,5- $d_2$  species of oxazole, but, despite intensive precautions, it was found impossible to prevent the occurrence of water in the reaction product, with a consequent, partial deuteration of the 2-position. Under optimum conditions, samples simultaneously enriched to between 15–30% in 4- $d_1$ , 5- $d_1$  and 2- $d_1$ -oxazole were obtained; normal oxazole ( $\sim 30\%$ ) and, doubtlessly, some poly-deuterated forms were also present, though the latter were not detected spectroscopically.

At room temperature, oxazole was found to decompose within a few days but, if kept below  $-30^\circ C$ , the compound proved to be quite stable.

#### b) Instrumental

Spectroscopic measurements were carried out in the frequency range from 10–40 GHz on a con-

Reprint requests to Dr. O. L. Stiefvater, School of Physical and Molecular Sciences, University College of North Wales Bangor LL57 2UW, Gwynedd, U.K.



Dieses Werk wurde im Jahr 2013 vom Verlag Zeitschrift für Naturforschung in Zusammenarbeit mit der Max-Planck-Gesellschaft zur Förderung der Wissenschaften e.V. digitalisiert und unter folgender Lizenz veröffentlicht: Creative Commons Namensnennung-Keine Bearbeitung 3.0 Deutschland Lizenz.

Zum 01.01.2015 ist eine Anpassung der Lizenzbedingungen (Entfall der Creative Commons Lizenzbedingung „Keine Bearbeitung“) beabsichtigt, um eine Nachnutzung auch im Rahmen zukünftiger wissenschaftlicher Nutzungsformen zu ermöglichen.

This work has been digitalized and published in 2013 by Verlag Zeitschrift für Naturforschung in cooperation with the Max Planck Society for the Advancement of Science under a Creative Commons Attribution-NoDerivs 3.0 Germany License.

On 01.01.2015 it is planned to change the License Conditions (the removal of the Creative Commons License condition “no derivative works”). This is to allow reuse in the area of future scientific usage.

ventional, Stark effect modulated (SEM) spectrometer [3] (modulation frequency: 100 kHz) with an X-band absorption cell of 3.5 m length. Free-running, frequency-swept klystrons were used as radiation sources, and absorptions were observed on the oscilloscope. Stark effect measurements were carried out at room temperature, and both the AC and the DC method for the displacement of Stark lobes were employed. Before and after each series of Stark effect measurements the absorption cell was calibrated against the lobes of the  $J = 0 \rightarrow 1$  or  $1 \rightarrow 2$  transitions of OCS, the dipole moment of which was taken as 0.71521 D [4].

Well-resolved hyperfine patterns of the low- $J$  transitions of oxazole were obtained at small power levels, low sample pressures, and with the absorption cell cooled to dry-ice temperature ( $-78^\circ\text{C}$ ).

### III. Results

#### a) Assignment of Spectra

The rotational spectrum of normal oxazole has been assigned in the initial study [5a] of oxazole and isoxazole, and the assignment of low- $J$  transitions, along with a preliminary analysis of hyperfine splittings, of the 2- $d_1$  species has been reported several years ago [5b]. Thus, while we now report extensions and refinements of these studies on the normal and the 2- $d_1$ -form, only the 4- $d_1$  and the 5- $d_1$  species remained for assignment in the present investigation. As in the case of the normal and 2- $d_1$  species, an assignment of these two forms was readily obtained from the  $J = 0 \rightarrow 1$  and  $J = 1 \rightarrow 2$  transitions, which were easily recognized by their resolved hyperfine splittings and Stark effects.

In view of the limited accuracy of rotational constants deduced from low- $J$  R-branch transitions alone, it was desirable to augment the assignments of the three mono-deuterated species through the identification of Q-branch transitions. Accordingly, the 2- $d_1$  and the 4- $d_1$  spectrum were studied up to  $J = 25$ . In the 5- $d_1$  species the inertial axis  $a$  approximately coincides with the direction of the dipole moment (see Part I, Figure 1) and Q-branch transitions could therefore be identified up to  $J = 9$  only.

As would be expected in a crowded spectrum, complicated by hyperfine splittings, the occurrence of excited vibration states and by the presence of up to four isotopic species in comparable concentra-

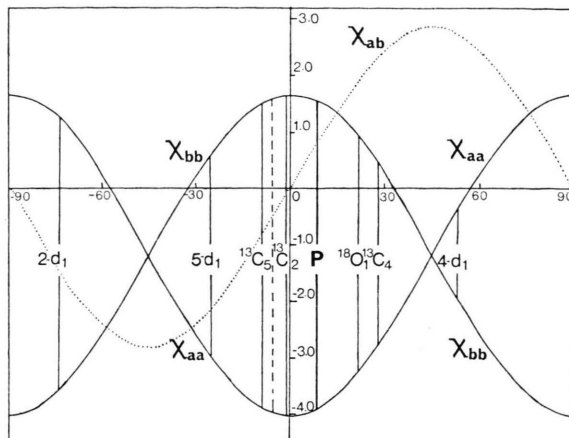


Fig. 1. Quadrupole coupling constants in oxazole as functions of the relative orientation of the inertial axes and the principal axes of the field gradient tensor.

tions, the consistency of Q-branch measurements by SEM spectroscopy fell somewhat short of the usual standards, and the assignment of a number of transitions with  $J > 10$  remained tentative. These shortcomings were readily rectified by DRM spectroscopy which yielded unequivocal Q-branch assignments up to  $J = 29$ , 25 and 24, respectively, for the 2- $d_1$ , 4- $d_1$  and 5- $d_1$  species (see Part I, Sections III b, c and Table 1).

#### b) Dipole Moment Measurements

The oxazole spectrum offers a good number of transitions which are suitable for a quantitative examination of their Stark effects. The  $J = 0 \rightarrow 1$  and  $J = 1 \rightarrow 2$  transitions, in particular, show intense and well resolved Stark lobes which can be linked unambiguously with individual components of the hyperfine multiplets. In all these cases, the Stark lobes associated with the strongest hyperfine component have been measured. For  $J > 3$  only transitions without hfs were chosen for the Stark effect analysis, and the  $M$ -values of individual lobes were ascertained in these cases through measurement of the displacement of at least three different lobes of the same transition in a given electric field. To determine the Stark coefficients ( $\Delta\nu/E^2$ ), between 10 and 20 measurements of the displacement  $\Delta\nu$  were taken at different electric field strengths  $E$  for each lobe studied. The coefficients  $A$  and  $B$  in the expression  $\Delta\nu = (A + BM^2) E^2$  for the frequency shift of the  $M$ th Stark lobe were calculated by the method of Golden and Wilson [6],

Table 1a. Comparison between observed and calculated Stark coefficients of the normal and mono-deuterated species of oxazole.

Transition			$\Delta\nu/E^2$ in MHz $10^6 (\text{V/cm})^{-2}$	
$J'_K - K'_K \leftarrow J_{K-K+}$	$F' \leftarrow F$	$M$	Observed	Calculated
<i>Parent form</i>				
$1_{01} - 0_{00}$	$2 - 1$	0	18.53	18.453
$1_{11} - 0_{00}$	$2 - 1$	0	10.68	10.453
$2_{11} - 1_{10}$	$3 - 2$	1	27.64	27.783
		0	3.78	3.645
$2_{12} - 1_{11}$	$3 - 2$	0	3.46	3.584
$3_{21} - 3_{22}$	a	3	6.15	6.171
		2	2.87	2.776
$6_{42} - 6_{43}$	a	6	1.48	1.478
		5	1.03	1.030
$6_{42} - 6_{33}$	a	6	1.18	1.143
		5	0.87	0.796
<i>2-d<sub>1</sub> species</i>				
$1_{11} - 0_{00}$	$2 - 1$	0	17.40	17.761
$1_{10} - 0_{00}$	$2 - 1$	0	11.54	11.765
$2_{02} - 1_{11}$	$3 - 2$	1	11.34	11.107
		0	3.53	3.442
$2_{12} - 1_{11}$	$3 - 2$	1	11.05	11.276
		0	3.40	3.395
$2_{12} - 1_{01}$	$3 - 2$	1	24.58	24.488
$2_{31} - 1_{10}$	$3 - 2$	1	29.50	29.387
$2_{11} - 1_{10}$	$3 - 2$	1	33.30	33.186
<i>4-d<sub>1</sub> species</i>				
$1_{11} - 0_{00}$	$2 - 1$	0	19.23	19.221
$2_{12} - 1_{01}$	$3 - 2$	1	27.66	27.658
		0	4.20	4.238
$2_{02} - 1_{11}$	$3 - 2$	1	7.05	7.064
<i>5-d<sub>1</sub> species</i>				
$2_{02} - 1_{01}$	$3 - 2$	1	4.90	4.850
$2_{12} - 1_{11}$	$3 - 2$	1	34.32	34.362
		0	5.70	5.484

a No hyperfine splitting.

and the dipole moment components were deduced from the observed Stark coefficients by least squares fits.

In the case of the *parent species* of oxazole eleven Stark lobes were studied on transitions up to  $J = 6$ , giving a total dipole moment of  $1.50 \pm 0.03$  D, oriented at an angle of  $24.8 \pm 1^\circ$  from the inertial axis  $a$ . The *2-d<sub>1</sub> species* also possesses comparable dipole components along both the  $a$  and  $b$  inertial axes, so that the same number of transitions as in the normal species should have been available for study. However, due to the limited enrichment ( $\sim 35\%$ ), Q-branch transitions were judged not intense enough for study of their Stark effects, and the dipole moment was therefore deduced from nine lobes of low- $J$  R-branch transitions only. The results indicated again a total moment of 1.50 D but with the orientation now deviating by  $59.8^\circ$  from the  $a$ -axis of this species. In the *4-d<sub>1</sub> species* the intensity of  $a$ -type transitions was found very small, indicating that the dipole moment now approximately coincided with the  $b$ -axis of the inertial tensor. As a result, the number of transitions suitable for the dipole determination was reduced to four, since the low enrichment ( $\sim 25\%$ ) did again not allow the study of Q-branch transitions. The results, nevertheless, showed satisfactory consistency, yielding a total moment of 1.51 D, inclined at an angle of  $69.4^\circ$  to the  $a$ -axis of this species. In the *5-d<sub>1</sub> species*, finally, the relative intensities of  $a$ - and  $b$ -type transitions were reversed in comparison to the *4-d<sub>1</sub> species*, permitting the study of only three Stark lobes on  $a$ -type

Species	Parent	2-d <sub>1</sub>	4-d <sub>1</sub>	5-d <sub>1</sub>
<i>Observed</i>				
1 $\mu_{\text{total}}$	1.503 (28)	1.501 (64)	1.510 (53)	1.485 (63)
2 $\alpha$	24.8 (10)	59.8 (24)	69.4 (20)	10.6 (24)
3 $\mu_a$	1.365 (20)	0.755 (50)	0.532 (50)	1.459 (20)
4 $\mu_b$	0.630 (20)	1.297 (40)	1.414 (20)	0.274 (60)
<i>Calculated</i>				
5 $\alpha^{\text{N}^a}$	...	57.4	69.5	8.7
6 $\mu_a^{\text{N}}$	...	0.809	0.527	1.485
7 $\mu_b^{\text{N}}$	...	1.266	1.407	0.227
8 $\alpha^0$	...	73.0	19.9	58.3
9 $\mu_a^0$	...	0.438	1.413	0.790
10 $\mu_b^0$	...	1.437	0.512	1.278

a  $\alpha^{\text{N},0}$  are the angles (in degrees) between the dipole moment and the  $a$ -axis calculated on the assumption that the dipole moment is oriented towards the nitrogen or the oxygen atom, respectively (see text and Figure 2).

Table 1b. Observed and calculated dipole components (in Debye units) of the normal and mono-deuterated species of oxazole.

transitions. The total moment of 1.49 D was found to deviate from the  $a$ -axis of this species by  $10.6^\circ$ .

A comparison between the observed and calculated Stark coefficients of transitions of the normal and the three mono-deuterated species of oxazole is given in Table 1a. Table 1b lists the values of the total dipole moment and its angle ( $\alpha$ ) with the  $a$ -axis in the four isotopic forms, as well as the observed dipole components along the principal axes. Rows 5–7 of this table give values of  $\alpha$ ,  $\mu_a$  and  $\mu_b$  calculated from the orientation of the moment of the normal species and the angles of rotation of the inertial axes under isotopic substitution (Part I, Table 1, row 3), together with the assumption that the dipole moment is oriented roughly from the centre of the ring towards the nitrogen atom. Rows 8–10 give the corresponding quantities but now calculated with the alternative assumption that the parent moment lies in the  $a$ - $b$ -quadrant containing the oxygen atom (see Figure 2).

Comparison of the experimental data (rows 1–4) with the results of these two calculations shows that the observed dipole components of the three mono-deuterated species are consistent only with the first assumption. The dipole moment of oxazole thus points from the centre of the ring towards the nitrogen end of the C(2)-N bond.

### c) Nuclear Quadrupole Coupling

Preliminary values of the quadrupole coupling constant in oxazole have been reported previously [5a, b]. The chief aims of the present study were

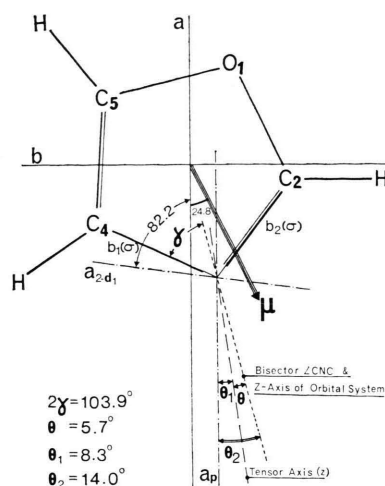


Fig. 2. Illustration of the axes and angles used in the analysis of the dipole and quadrupole data of oxazole.

therefore, firstly, to finalise the earlier data through improved accuracy and, secondly, to extend the investigation to different isotopic species in order to deduce the principal values of the coupling tensor and its orientation with respect to the inertial axes; in conjunction with the known geometry (Part I) of oxazole this would also allow the orientation of the tensor with respect to the ring bonds between the nitrogen atom and the adjacent carbons to be determined. Accordingly, the hyperfine splittings of ten well-resolved transitions of the parent species and of seven transitions of the 2- $d_1$  species were measured (Table 2a) and, by application of the standard

Species	Transition	Hyperfine splitting $\Delta\nu_{12}$			
	$J'_{K'-K+} \leftarrow J_{K-K+}$	$F_1' \leftarrow F_1$	$F_2' \leftarrow F_2$	Measured	Calculated
Parent	$1_{01} - 0_{00}$	$2 - 1$	$1 - 1$	1.162	1.176
		$0 - 1$	$2 - 1$	2.942	2.940
		$0 - 1$	$1 - 1$	1.780	1.764
	$1_1 - 0_{00}$	$2 - 1$	$0 - 1$	0.701	0.693
		$1 - 1$	$0 - 1$	1.163	1.155
		$1 - 1$	$2 - 1$	0.462	0.462
	$2_{02} - 1_{01}$	$3 - 2$	$2 - 2$	0.923	0.835
		$3 - 2$	$1 - 0$	1.374	1.300
		$2 - 1$	$3 - 2$	0.405	0.341
		$2 - 2$	$1 - 0$	0.452	0.465
	$2_{12} - 1_{11}$	$3 - 2$	$2 - 1$	1.182	1.227
		$1 - 0$	$2 - 1$	2.457	2.345
		$1 - 0$	$3 - 2$	1.274	1.118
	$2_{11} - 1_{10}$	$3 - 2$	$2 - 1$	1.178	1.209
		$1 - 0$	$3 - 2$	1.368	1.346

Table 2a. Comparison between observed and calculated hyperfine splittings of the normal and the three mono-deuterated species of oxazole.



Table 2a (continued)

Species	Transition	Hyperfine splitting $\Delta\nu_{12}$			
		$J'_{K-K_+} \leftarrow J_{K-K_+}$	$F_1' \rightarrow F_1$	$F_2' \rightarrow F_2$	Measured      Calculated
2-d <sub>1</sub> species	$2_{12} - 1_{01}$	3-2	1-0		1.336      1.339
		1-1	1-0		2.945      2.940
		3-2	2-2		0.910      0.765
	$2_{02} - 1_{11}$	1-1	3-2		1.608      1.601
		3-2	2-1		1.269      1.297
		1-0	2-1		2.376      2.454
	$2_{21} - 1_{10}$	1-0	3-2		1.107      1.157
		3-2	1-1		1.478      1.414
		2-2	1-1		2.700      2.674
	$2_{21} - 2_{02}$	2-2	3-2		1.252      1.260
		3-3	1-1		1.251      1.164
		2-2	3-3		2.133      2.095
	$2_{12} - 2_{21}$	2-2	1-1		3.385      3.259
		3-3	1-1		1.065      1.125
		2-2	3-3		2.005      2.025
		2-2	1-1		3.070      3.150
	$1_{01} - 0_{00}$	2-1	0-1		0.569      0.549
		1-1	0-1		0.916      0.915
		1-1	2-1		0.347      0.366
	$1_{11} - 0_{00}$	2-1	1-1		1.060      1.08
		0-1	2-1		1.640      1.620
		0-1	1-1		2.700      2.700
	$2_{12} - 1_{11}$	3-2	2-2		0.770      0.765
		2-1	2-2		1.080      1.080
		3-2	1-0		1.190      1.195
	$2_{12} - 1_{01}$	2-1	1-0		1.508      1.510
		2-1	3-2		0.310      0.315
		2-2	1-0		0.420      0.430
	$2_{21} - 1_{10}$	3-2	2-1		1.114      1.131
		1-0	3-2		0.966      0.974
		1-0	2-1		2.080      2.105
	$2_{11} - 1_{10}$	1-0	3-2		1.276      1.289
		1-0	1-1		1.800      1.785
		3-2	2-1		1.250      1.106
	$2_{02} - 1_{11}$	3-2	1-1		1.354      1.356
		2-2	3-2		1.106      1.158
		3-2	1-0		1.242      1.236
4-d <sub>1</sub> species	$1_{11} - 0_{00}$	3-2	2-2		0.668      0.690
		1-1	3-2		1.432      1.464
		1-1	1-0		2.674      2.700
	$2_{12} - 1_{01}$	1-1	2-2		2.100      2.154
		2-1	1-1		0.530      0.600
		0-1	2-1		0.830      0.900
	$2_{12} - 1_{01}$	0-1	1-1		1.360      1.500
		3-2	2-1		0.656      0.652
		1-1	3-2		0.484      0.537
	$2_{02} - 1_{11}$	3-2	1-0		0.504      0.507
		1-1	3-2		1.076      1.001
		1-1	1-0		1.580      1.508
5-d <sub>1</sub> species	$2_{21} - 1_{10}$	3-2	1-1		0.756      0.780
		1-0	3-2		1.056      1.008
		1-0	1-1		1.812      1.788
	$2_{11} - 1_{10}$	3-2	2-1		0.792      0.906
		1-0	3-2		1.210      1.178
		1-0	2-1		2.002      1.084
	$2_{02} - 1_{01}$	3-2	2-2	} 0.888	0.869
		3-2	1-0		0.871
		1-1	3-2		1.428      1.384
	$2_{12} - 1_{11}$	3-2	2-1		0.952      0.950
		1-0	3-2		0.750      0.702
		1-0	2-1		1.702      1.652

Table 2b. Observed and calculated quadrupole coupling constants of the normal and the three mono-deuterated species of oxazole (in MHz).

	Parent form	2-d <sub>1</sub> species	4-d <sub>1</sub> species	5-d <sub>1</sub> species	Principal values
<i>Observed</i>					
$\chi_{aa}$	−3.92 (2) <sup>a</sup>	1.22 (2) <sup>a</sup>	−0.37 (5)	−2.98 (5)	....
$\chi_{bb}$	1.54 (2) <sup>a</sup>	−3.60 (2) <sup>a</sup>	−2.01 (5)	0.60 (5)	....
$\chi_{cc}$	2.38	2.38	2.38	2.38	....
<i>Calculated</i>					
$\chi_{aa}$	a	a	−0.34	−3.00	−4.04
$\chi_{bb}$	a	a	−2.04	0.62	1.66
$\chi_{ab}$	0.81	−1.52	2.74	−2.19	0.0

<sup>a</sup> Values used for the determination of the principal tensor (last column).

theory [7], the coupling constants for these two species were deduced to within  $\pm 0.02$  MHz by least squares fits of  $\chi_{aa}$  and  $\chi_{bb}$ , with  $\chi_{cc}$  deduced from the Laplace equation. As in the dipole moment study (Section b, above) the number of transitions suitable for examination of hyperfine splittings in the 4-d<sub>1</sub> and 5-d<sub>1</sub> species was reduced on account of the smaller isotopic enrichment and the less favourable orientation of the dipole moment (*b*-type or *a*-type transitions only). Hence, only three and four transitions, respectively, could be studied in these two species, yielding coupling constants to an accuracy of  $\pm 0.05$  MHz.

For a planar molecule such as oxazole, the field gradients along the “in-plane” inertial axes (*a*, *b*) of different isotopic species are related simply by a rotation of the coordinate system (inertial axes), while the gradient perpendicular to the molecular plane remains unchanged by isotopic substitution, and is equal to a principal value of the field gradient tensor. Hence, from the measured  $\chi$ -values of the normal and the 2-d<sub>1</sub> species of oxazole, and in conjunction with the known angle of rotation (82.2°) of the inertial axes under substitution of H(2) (Part I, Table 1, row 3), the off-diagonal element  $\chi_{ab}$  of the field gradient tensor of the parent species was deduced as

$$\chi_{ab} = 0.81 \text{ MHz.}$$

Through diagonalisation of the completely known field gradient tensor of the parent species, the principal values of this tensor were thus obtained as

$$\begin{aligned}\chi_{zz} &= -4.04 \text{ MHz,} \\ \chi_{xx} &= 1.66 \text{ MHz,} \\ \chi_{yy} = \chi_{cc} &= 2.38 \text{ MHz}\end{aligned}$$

resulting in an asymmetry parameter

$$\eta = (\chi_{xx} - \chi_{yy})/\chi_{zz} = +0.178$$

and indicating that the direction of the largest field gradient (*z*-axis) deviates by

$$\theta_1 = (1/2) \arctan \{ (2\chi_{ab})/(\chi_{bb} - \chi_{aa}) \} = 8.3^\circ$$

from the inertial axis *a* of the parent species. These data, in turn, allowed the prediction of the coupling constants for all isotopic species (Fig. 1 and Part I, Table 1, row 5), as well as a cross-check against the observed  $\chi$ -values of the 4-d<sub>1</sub> and 5-d<sub>1</sub> species (Table 2b). Moreover, from the structure data of Part I, and the precise knowledge of the angle  $\theta_2$  between the bisector of the CNC-angle ( $2\gamma = 103.9^\circ$ ) and the inertial axis *a* of the parent species, in particular, the above data also permitted the deviation of the *z*-axis of the field gradient tensor from the external bisector of the CNC-angle to be determined as  $5.7^\circ$  towards the C(4) atom (see Figure 2).

The electric field gradients, which become detectable through their interaction with a quadrupolar nucleus, arise from the non-spherical distribution of the surrounding valency electrons and it is, therefore, the prime purpose of the study of quadrupole couplings in molecules to interpret the orientation and magnitude of the measured field gradient tensor in terms of the occupation of the bonding orbitals, and thus to deduce information about the electron densities in the bonds emanating from the quadrupolar atom. Though first formulated by Townes and Dailey [8], the quantum chemical concepts for correlating observed  $\chi$ -values with the occupation of particular atomic orbitals have been elucidated and discussed by Lucken [9], whose treatment is now widely adopted.

Accordingly, following Lucken's scheme for converting the observed orientation and magnitude of the field gradients in oxazole into information about the orbital populations of the  $sp^2$ -hybridised nitrogen atom, the principal gradients  $\chi_{xx}$ ,  $\chi_{yy}$  and  $\chi_{zz}$  were first resolved along the orbital axis system ( $X, Y, Z$ ), the  $Z$ -axis of which is taken coincident with the external bisector of the CNC bond angle (see Fig. 2), to give:

$$\begin{aligned}\chi_{zz} &= -3.98 \text{ MHz}, \\ \chi_{xx} &= 1.60 \text{ MHz}, \\ \chi_{yy} = \chi_{yy} = \chi_{cc} &= 2.38 \text{ MHz},\end{aligned}$$

$$\text{and } \eta' = (\chi_{xx} - \chi_{yy})/\chi_{zz} = +0.196.$$

The populations  $a(\pi)$ ,  $b_1(\sigma)$  and  $b_2(\sigma)$  of the  $\pi$ -orbital and of the  $\sigma$ -orbitals contributing to the N(3)–C(4) and the N(3)–C(2) bonds, respectively, where then calculated from the relations (9):

$$\begin{aligned}(1/2)(b_1 + b_2 - 2a) &= (2/3) \eta' (\chi_{zz}/\chi_p), \\ (1/2)(4 - (b_1 + b_2)) \\ &= (1 - \cot^2 \gamma)^{-1} (1 - (\eta'/3)) (\chi_{zz}/\chi_p),\end{aligned}$$

$$\text{and } (b_1 - b_2)/(4 - b_1 - b_2) = \tan 2\theta/\tan 2\gamma$$

where  $\theta = \theta_1 - \theta_2$

is the deviation of the direction of the largest field gradient from the external bisector of the CNC angle ( $Z$ -axis). With the field gradient produced by a single unbalanced 2p electron taken as  $\chi_p = -10.0$  MHz, Lucken's equations gave the population numbers as:  $a(\pi) = 0.988$ ,  $b_1(\sigma) = 0.992$  and  $b_2(\sigma) = 1.088$ .

## IV. Discussion

### a) Dipole Moment

In analogy with the view taken by previous workers [10], the dipole moment of oxazole may be interpreted as the vector sum of a moment  $\mu_N$ , associated with the pyridine-like nitrogen atom, and a contribution  $\mu_{\text{resid.}}$  describing the polarity of the residual ring structure. While the dipole moment (0.66 D) of furan [11], taken along the COC bisector with the oxygen atom negative with respect to the ring [12], would appear to provide a safe estimate for  $\mu_{\text{resid.}}$ , it has been found in the case of thiazole [10] that an apparently good indication of  $\mu_N$  was obtained when the dipole moment (2.23 D) of pyridine [13] was scaled by the ratio of the  $\chi_{zz}$ -values of thiazole and pyridine.

Proceeding in a corresponding manner, we find in the case of oxazole that, depending on whether  $\mu_N = 1.85$  D is chosen along the CNC bisector or along the  $\chi_{zz}$ -direction, the vector sum of  $\mu_N$  and  $\mu_{\text{resid.}}$  is 0.10 D or 0.16 D smaller than the observed moment, and that its direction deviates by  $+6.5^\circ$  or  $-1.0^\circ$ , respectively, from the observed value. In either case, the agreement between the vector sum and the moment of oxazole is noticeably worse than in thiazole, where no ambiguity about the direction of the assumed  $\mu_N$  can arise since the  $\chi_{zz}$ -direction virtually coincides with that of the CNC bisector (Table 3, column I, rows 5a and 6a).

Since the major part of the stated discrepancy between the vector sum of estimated contributions and the observed moment of oxazole arises, most probably, from erroneous assumptions about  $\mu_N$ , we thought it more appropriate to determine  $\mu_N$  by vectorial subtraction of the assumed  $\mu_{\text{resid.}}$  from the observed moment of oxazole. By this approach, one obtains  $\mu_N = 1.99$  D, inclined to the  $a$ -axis by  $10.2^\circ$ , and hence deviating from the CNC bisector in the same direction as  $\chi_{zz}$ , from which it differs by  $2^\circ$ . Furthermore, by application of the same idea in related compounds (Table 3) it is found that the magnitude of the  $\mu_N$ -values thus deduced is in qualitative agreement with the values derived from the previously assumed relation

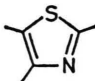
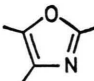
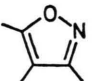
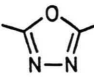
$$\mu_N = \mu_{\text{pyrid.}} (\chi_{zz}/\chi_{zz,\text{pyrid.}}),$$

while the direction of  $\mu_N$  is noticeably closer to that of  $\chi_{zz}$  than to the direction of the bisector (compare row 2 with 3a, and row 3c = row 5a – row 3b of Table 3). This, in turn, suggests that  $\mu_N$  shares with  $\chi_{zz}$  the property of indicating the approximate orientation of the lone pair orbital of the nitrogen atom. Not surprisingly, the largest discrepancy between the direction of  $\mu_N$  and  $\chi_{zz}$  occurs for isoxazole [14], where the assumption of a constant  $\mu_{\text{resid.}}$ , directed along the CON bisector, would seem to be much less justifiable than in the other three cases, because of the adjacency of different atoms.

### b) Quadrupole Coupling Constants

The quadrupole data for oxazole are compared with their counterparts in thiazole [10], isoxazole [14] and 1,3,4-oxadiazole [15] in rows 4–7 of Table 3. All three principal coupling constants of oxazole are about 10% smaller than their equiva-

Table 3. Comparison between the dipole moments (in Debye), quadrupole coupling constants (in MHz) and structure parameters (in Å) of oxazole and related compounds.

	I Thiazole ref. 10	II Oxazole This study	III Isoxazole ref. 14	IV 1,3,4-oxadiazole ref. 15	
					
<i>Dipole moment</i>					
1 a	$\mu_{\text{observed}}$	1.61	1.50	2.90	3.04
1 b	$\angle (\mu_{\text{obs.}}, a\text{-axis})$	36.9°	24.8°	~47°	0
2	$\mu_{\text{N}} = (\mu/\chi_{\text{zz}})_{\text{pyrid.}} \times \chi_{\text{zz}}$	2.02	1.85	2.46	1.93
3 a	$ \mu_{\text{N}}  =  \mu_{\text{obs.}} - \mu_{\text{resid.}} $	2.05	1.99	2.46	1.98 (2.23) <sup>a</sup>
3 b	$\angle (\mu_{\text{N}}, a\text{-axis})$	27.1°	10.2°	36.4°	21.2° (37.2°) <sup>a</sup>
3 c	$\angle (\mu_{\text{N}}, \chi_{\text{zz}}\text{-axis})$	+4.8°	−2.0°	+11.6°	0 (16.0°) <sup>a</sup>
<i>Quadrupole coupling data</i>					
Inertial axis system (a, b, c)					
4 a	$\chi_{\text{aa}}$	−2.670	−3.92	0.526	−3.80
4 b	$\chi_{\text{bb}}$	0.085	1.54	−0.609	2.02
4 c	$\chi_{\text{cc}}$	2.585	2.38	0.083	1.78
4 d	$\chi_{\text{ab}}$	2.80	0.81	5.35	2.65
Principal axis system (x, y, z)					
5 a	$\theta_1 = \angle (z\text{-axis}, a\text{-axis})$	31.9°	8.3°	48°	21.2°
5 b	$\chi_{\text{zz}}$	−4.41	−4.04	−5.39	−4.83
5 c	$\chi_{\text{xx}}$	1.83	1.66	5.37	3.05
5 d	$\chi_{\text{yy}} = \chi_{\text{cc}} = \chi(\perp)$	2.585	2.38	0.02	1.78
Orbital axis system (X, Y, Z)					
6 a	$\theta_2 = \angle (\text{CNC bisect.}, a\text{-axis})$	31.5°	14.0°	21.9°	37.2°
6 b	$\theta = \theta_1 - \theta_2$	0.4°	5.7°	26.1°	16.0°
6 c	$2\gamma = \text{bond angle at N-atom}$	110.1°	103.9°	105.3°	105.6°
7 a	$\chi_{\text{zz}}$	−4.41	−3.98	−3.31	−4.23
7 b	$\chi_{\text{xx}}$	1.83	1.60	3.29	2.45
7 c	$\chi_{\text{yy}} = \chi(\perp)$	2.58	2.38	0.02	1.78
<i>Orbital populations and ionic character</i>					
8 a	$a(\pi)$	1.137	0.988	1.165	0.994
8 b	$b_1(\sigma) = \text{N} - \text{X bond}$	1.183	0.992	0.578	0.766
8 c	$b_2(\sigma) = \text{N} = \text{C bond}$	1.191	1.088	1.316	1.133
8 d	$c = i_{\pi} + i_{\sigma} = a + b_1 + b_2 - 3$	0.511	0.068	0.059	−0.107
<i>Structure data</i>					
9 a	distance 1,2	S−C: 1.724	O−C: 1.357	O−N: 1.399	O−C: 1.348
9 b	distance 2,3	C−N: 1.304	C−N: 1.292	N−C: 1.309	C−N: 1.297
9 c	distance 3,4	N−C: 1.372	N−C: 1.395	C−C: 1.425	N−N: 1.399
9 d	distance 4,5	C−C: 1.367	C−C: 1.353	C−C: 1.356	N−C: 1.297
9 e	distance 5,1	C−S: 1.713	C−O: 1.370	C−O: 1.344	C−O: 1.348

<sup>a</sup> These values are obtained from the *assumption* that the direction of  $\mu_{\text{N}}$  coincides with the z-axis (compare row 5a). The values in parenthesis would be obtained if  $\mu_{\text{N}}$  was assumed along the CNN bisector (see row 6a).

lents in thiazole, but they differ considerably from their counterparts in isoxazole and 1,3,4-oxadiazole. In the latter two substances the field gradient of smallest magnitude lies in a direction perpendicular to the molecular plane (direction of the  $\pi$ -orbital), while oxazole and thiazole have their smallest gradient in the molecular plane and perpendicular

to the likely direction of the nitrogen lone pair orbital. Also, in oxazole and thiazole the deviation of the in magnitude largest field gradient from the bisector of the bond angle at the nitrogen atom is small in comparison with the deviations in isoxazole and 1,3,4-oxadiazole (row 6b of Table 3). Both these observations suggest that the nitrogen atom



in oxazole and thiazole is essentially like that in pyridine, with the gradient perpendicular to the molecular plane reduced by  $\sim 30\%$ , and the gradient perpendicular to the lone pair orbital increased by  $\sim 20\%$  in comparison with pyridine ( $\chi_{zz} = -4.87$  MHz,  $\chi_{xx} = 1.40$  MHz,  $\chi_{yy} = \chi(\perp) = 3.47$  MHz). This similarity between the hybridisation state of the nitrogen atom in pyridine, on the one hand, and in oxazole and thiazole, on the other, naturally also becomes apparent in the orbital populations (rows 8 of Table 3) as deduced from the coupling constants by Lucken's method. Thus, the relative magnitudes of the  $\pi$ - and  $\sigma$ -populations in oxazole and thiazole remain essentially the same as in pyridine, although the two C-N bonds now contain unequal  $\sigma$ -populations. Together with the smaller  $\pi$ -populations, this probably has to be taken as a manifestation of the reduced aromaticity in comparison with pyridine. While still comparable in oxazole and thiazole, the two  $\sigma$ -populations (rows 8b, 8c) in isoxazole and 1,3,4-oxadiazole differ considerably from each other and from the pyridine value ( $b(\sigma) = 1.331$ ). As with the modification of the principal coupling constants themselves, this is most probably the result of there being two chemically different atoms adjacent to the coupling nucleus, entailing differing amounts of ionic character in the ring bonds to the nitrogen atom.

Comparison of the field gradients should also be made with the earlier, semi-empirical calculations of Davies and Mackrodt [16] and with the *ab initio* work of Kochanski, Lehn and Levy [17]. Unfortunately, Davies and Mackrodt give the calculated coupling constants only with respect to the (unstated) inertial axes of model structures, the precision of which was not known at the time of their calculations. Hence, in comparing their predictions with the experimental values, allowance must be made not only for the uncertainty in the value of  $\chi_p$ , but also for the uncertainty in the angle  $\theta_1$  which they used in the transformation of the principal field gradients. In view of the sensitivity of the orientation of the inertial axes to small changes in the model structure, the error in  $\theta_1$  might have been appreciable. Nevertheless, both the signs and the magnitudes of the coupling constants calculated by Davies and Mackrodt agree to within 15% with the experimental values for the parent form of oxazole.

In comparison with the semi-empirical approach [16], the principal coupling constants obtained from *ab initio* calculations by Kochanski, Lehn and Levy [17] should be less sensitive to inaccuracies in the assumed molecular structure. In our axis notation, the results of this work for oxazole are:

$$\begin{aligned}\chi_{zz} &= -4.98 \text{ MHz,} \\ \chi_{xx} &= +3.41 \text{ MHz,} \\ \chi_{yy} = \chi_{cc} = \chi(\perp) &= +1.57 \text{ MHz}\end{aligned}$$

with the  $z$ -direction roughly along the bisector of the CNC angle. Hence, from a comparison with the observed values (Table 3, rows 5b–d), it is seen that, while  $\chi_{zz}$  is reasonably well predicted, the observed gradient  $\chi_{yy}$  perpendicular to the molecular plane ( $\pi$ -direction) is larger than  $\chi_{xx}$  which, erroneously, had been correlated with the calculated gradient in the  $\pi$ -direction (Ref. [17], Table 1, compound V). The experimental results for oxazole and thiazole thus contradict the suggested generalisation [17] that the smallest  $\chi$ -component would lie in the direction of the  $\pi$ -system for all di-coordinated nitrogen atoms.

### c) Molecular Structure

A quantitative correlation between the electron distribution, as apparent through the dipole and quadrupole data of the present study, and the molecular structure reported in the previous part [1], is not easily detected. This, of course, is not surprising when one considers that the dipole contribution  $\mu_N$  and the information derived from the quadrupole coupling constants concern only the immediate vicinity of the nitrogen atom, whereas the electron distribution around the other four ring atoms, and especially around the second hetero atom O(1), remains unexplored in our experiment. Nevertheless, the previous conclusion (Part I, Sect. V) that the interchange of the carbon and nitrogen positions between oxazole and isoxazole must be accompanied by a significant change of the electron distribution around the nitrogen atom is fully borne out in the values for the  $\pi$ - and  $\sigma$ -populations of oxazole, which differ considerably from those of isoxazole (Table 3, columns II and III, rows 8a–8c); the large populations of the  $\pi$ -orbital and of the  $\sigma$ -orbital involved in the C=N bond of isoxazole indicate a smaller ionicity of the carbon atom C(3). By comparison of all four compounds listed in Table 3

it is also noticed that the length of the carbon-nitrogen double bonds appear correlated with both the  $a(\pi)$  and  $b_2(\sigma)$ -values in such a way that the highest population values occur with the largest C=N bond length (compare Table 3, rows 8a and 8c with 9b). These comparisons suggest that delocalisation at the nitrogen atom increases along the series isoxazole, thiazole, 1,3,4-oxadiazole, although Zeeman work seems to indicate that the aromatic character of oxazole and isoxazole is similar [18].

Finally, it is worth noting that the C=C bonds in oxazole and isoxazole are virtually unaffected by the changes in the electron distribution around the nitrogen atom, and that the lengths of the formal

single bond emanating from the nitrogen atom are the same in oxazole, isoxazole and 1,3,4-oxadiazole and apparently independent of the atom connection (C-N, O-N, N-N, respectively), as anticipated by Nygaard and collaborators [15].

#### Acknowledgement

We acknowledge the gift of oxazole samples by Professor H. Brederick and Dr. K. H. W. Turck, and we thank the S.R.C. for a Research Support Grant. A.K. would like to thank the Leverhulme Trust for a Commonwealth Visiting Fellowship and the University College of North Wales for a Research Fellowship. We thank Mr. D. H. Owen for carrying out the sample preparations.

- [1] A. Kumar, J. Sheridan, and O. L. Stiefvater, *Z. Naturforsch.* **33a**, 145 (1978).
- [2] a) R. Bangert, Dissertation, T. H. Stuttgart, 1963. b) H. Brederick and R. Bangert, *Angew. Chem.* **74**, 905 (1962).
- [3] R. H. Hughes and E. B. Wilson, jr. *Phys. Rev.* **71**, 562 (1947).
- [4] J. S. Muentner, *J. Chem. Phys.* **48**, 4544 (1968).
- [5] a) W. C. Mackrodt, A. Wardley, P. A. Curnuck, N. L. Owen, and J. Sheridan, *J. C. S. Chem. Comm.* 692 (1966). b) A. Wardley and J. Sheridan, *I. Europ. Microwave Spectroscopy Conference Bangor, Wales 1970* (Paper A1-5).
- [6] S. Golden and E. B. Wilson, jr., *J. Chem. Phys.* **16**, 699 (1948).
- [7] a) C. H. Townes and A. L. Schawlow, *Microwave Spectroscopy*, McGraw Hill Book Co., New York 1955. b) W. Gordy and R. L. Cook, *Microwave Molecular Spectra*, Interscience Publishers 1970.
- [8] C. H. Townes and H. P. Dailey, *J. Chem. Phys.* **17**, 782 (1949).
- [9] E. C. A. Lucken, *Nuclear Quadrupole Coupling Constants*, Academic Press, London 1969.
- [10] L. Nygaard, F. Asmussen, J. H. Høg, R. C. Maheshwari, C. H. Nielsen, I. B. Petersen, J. Rastrup-Andersen, and G. O. Sørensen, *J. Mol. Struct.* **8**, 225 (1971).
- [11] B. Bak, W. B. Dixon, D. Christensen, L. Hansen-Nygaard, J. Pastrup-Andersen, and M. Schottländer, *J. Mol. Spectrosc.* **9**, 124 (1962).
- [12] T. J. Barton, R. W. Roth, and J. G. Verkade, *J. Amer. Chem. Soc.* **94**, 8854 (1972).
- [13] a) B. Bak, L. Hansen-Nygaard, and J. Rastrup-Andersen, *J. Mol. Spectrosc.* **2**, 361 (1958). b) G. O. Sørensen, *J. Mol. Spectrosc.* **22**, 325 (1967).
- [14] a) O. L. Stiefvater, P. Nösberger, and J. Sheridan, *Chem. Phys.* **9**, 435 (1975). b) O. L. Stiefvater, *J. Chem. Phys.* **63**, 2569 (1975). c) S. Lowe and J. Sheridan, to be published.
- [15] L. Nygaard, R. L. Hansen, J. T. Nielsen, J. Rastrup-Andersen, G. O. Sørensen, and P. A. Steiner, *J. Mol. Struct.* **12**, 59 (1972).
- [16] D. W. Davies and W. C. Mackrodt, *J. C. S. Chem. Comm.* 1226 (1967).
- [17] E. Kochanski, J. M. Lehn, and B. Levy, *Theoret. Chim. Acta*, **22**, 111 (1971).